JACS
JOURNAL OF THE AMERICAN CHEMICAL SOCIETY

ARTICLE

pubs.acs.org/JACS

Chiral 1,2-Subnaphthalocyanines

Soji Shimizu,[†] Akito Miura,[†] Samson Khene,[‡] Tebello Nyokong,*[,‡] and Nagao Kobayashi*[,†]

[†]Department of Chemistry, Graduate School of Science, Tohoku University, Sendai 980-8578, Japan

[‡]Department of Chemistry, Rhodes University, Grahamstown 6140, South Africa

Supporting Information

ABSTRACT: Following the first suggestion of inherent molecular chirality in asymmetrically substituted subphthalocyanines by Torres and co-workers in 2000, elucidation of the relationship between structure and chirality has become an important issue. However, separation of the enantiomers has been prevented by the low solubility of the molecules synthesized to date, and it has not been possible to link the CD signs and intensities to their absolute structures. Recently, we observed that 1,2-subnaphthalocyanines possess two diastereomers with respect to the arrangement of the naphthalene moieties and that these novel chiral molecules exhibit moderate solubility in common organic solvents. This has enabled us to separate all of the diastereomers and enantiomers. The two diastereomers have been completely characterized by NMR spectroscopy and X-ray diffraction analysis. The absorption and magnetic circular dichroism spectra, together with theoretical calculation, reveal a small variation in the frontier molecular orbitals of the 1,2-subnaphthalocyanines compared with conventional subphthalocyanines, except for destabilization of the HOMO−3, which results in a characteristic absorption in the Soret band region. The chirality of 1,2-subnaphthalcyanines, including the CD signs and intensities, is discussed in detail for the first time with enantiomerically pure molecules whose absolute structures have been elucidated by single-crystal X-ray diffraction analysis.

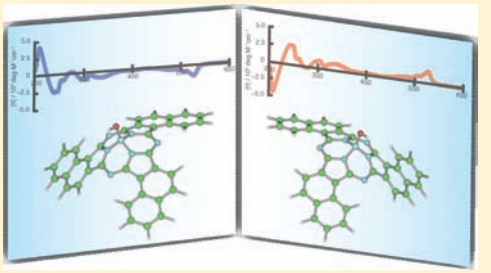

INTRODUCTION

Subphthalocyanine (SubPc) is a ring-contracted congener of phthalocyanine (Pc), comprising three isoindole units linked by three nitrogen atoms.[1] As a result of its C_{3v}-symmetric bowl-shaped structure[2] with a boron atom at the center and its 14π-electron aromatic conjugation system, SubPc exhibits unique optical properties, such as strong absorption in the UV/vis region, intense fluorescence with moderate quantum yields, and unique nonlinear optical properties.[3,4] The central boron atom plays a crucial role in maintaining the bowl-shaped structure, as well as enabling further functionalization by linking other functional units at the axial position.[5] Due to the proximity of their LUMO energy levels, hybrid materials of SubPc and C_{60} have been the subject of increasing interest in the fields of organic solar cells[6] and organic transistor devices,[7] and the photoinduced energy- and electron-transfer processes of SubPc−C_{60} conjugates have been intensively investigated.[8,9] The bowl-shaped molecular structure of SubPc is also beneficial for constructing supramolecular architectures with fullerenes, both in solution[10] and in the solid state.[11] Another unique property arising from the structural features is an inherent molecular chirality when a SubPc molecule is asymmetrically substituted, which was first suggested by Torres and Claessens.[12] From reactions of asymmetrically substituted phthalonitriles, such as 4-iodophthalonitrile[12a] and 3-nitro-5-*tert*-butylphthalonitrile,[13] two structural isomers having C_3 and C_1 molecular symmetries with respect to the arrangement of the substituents were obtained, with each structural isomer being inherently chiral due to the absence of any mirror plane in their structures. This inherent chirality of the asymmetrically substituted SubPc can be regarded as a type of "bowl chirality",[14] which has been of intense interest in the fields of fullerenes[15] and carbon nanotubes,[16] since molecules containing three-dimensional chiral π-surfaces can provide a space for molecular recognition and asymmetric catalytic reactions. Although the use of chiral SubPcs for these applications has been strongly anticipated, its chemistry is still at an early stage, with little general information being available on the relationship between the absolute molecular structures and the signs and intensities of their circular dichroism (CD) spectra. Quantum chemical calculation is a useful tool for predicting the structure−chirality relationship to a certain extent,[17] but in a general sense, elucidation of an absolute structure by single-crystal X-ray diffraction analysis based on the Bijvoet method[18] is much more straightforward. However, in the previous studies, the low solubility and small structural difference of the diastereomers has prevented complete separation and characterization of all of the diastereomers and enantiomers.[12,13] For further study of the structure−chirality relationship, SubPc molecules with moderate solubility in common organic solvents and with small variations in optical properties are required. 1,2-Naphthalocyanines[19] synthesized from 1,2-naphthalenedicarbonitrile are known to exist as four structural isomers having C_{4h}, C_{2v}, C_s, and D_{2h} symmetries with respect to the arrangement of the peripheral

Received: June 7, 2011
Published: October 07, 2011

benzene rings, but the changes in positions and shapes of the Q-band absorption from those of Pcs are small, except for the D_{2h} isomer.[19b] This prompted us to synthesize novel chiral SubPc molecules by using a 1,2-naphthalene unit as a key building block. The aim of this study was to separate all of the diastereomers and enantiomers of 1,2-subnaphthalocyanines (1,2-SubNcs) and determine their absolute structures by X-ray analysis, which has enabled a comprehensive understanding of the structure−chirality relationship of inherently chiral SubPcs.

EXPERIMENTAL SECTION

General Procedure. Electronic absorption spectra were recorded on a JASCO V-570 spectrophotometer. CD and magnetic circular dichroism (MCD) spectra were recorded on a JASCO J-725 spectropolarimeter equipped with a JASCO electromagnet, which produces magnetic fields of up to 1.09 T (1 T = 1 tesla) with both parallel and antiparallel fields. The magnitudes were expressed in terms of molar ellipticity ($[\theta]$/deg dm^3 mol^{-1} cm^{-1}) and molar ellipticity per tesla ($[\theta]_M$/deg dm^3 mol^{-1} cm^{-1} T^{-1}), respectively. Fluorescence spectra were measured on a Hitachi F-4500 spectrofluorimeter. ^{1}H NMR spectra were recorded on a JEOL ECA-600 spectrometer (operating as 594.17 MHz for ^{1}H) and a Bruker AVANCE 400 spectrometer (operating at 400.33 MHz) using the residual solvent as the internal reference for ^{1}H (δ = 7.260 ppm for $CDCl_3$). High resolution mass spectra were recorded on a Bruker Daltonics Apex-III spectrometer. Preparative separations were performed by silica gel column chromatography (Merck Kieselegel 60H for thin layer chromatography). Separation of all the enantiomers was carried out by high-performance liquid chromatography (HPLC) with a preparative CHIRALPAK IA column by monitoring absorbance at 520 nm.

Crystallographic Data Collection and Structure Refinement. Data collection was carried out at −100 °C on a Rigaku Saturn CCD spectrometer with Mo Kα radiation (λ = 0.71070 Å) for **1c** and **2c** and at −173 °C on a Bruker APEXII CCD diffractometer with Mo Kα radiation (λ = 0.71073 Å) for **1dFr1**. The structures were solved by a direct method (SHLEXS-97)[20] and refined using a full-matrix least-squares technique (SHELXL-97).[20] CCDC-828217, -828218, and -828219 contain the supplementary crystallographic data for **1c**, **2c**, and **1dFr1**, respectively. These data can be obtained free of charge from the Cambridge Crystallographic Data Centre via www.ccdc.cam.ac.uk/data_request/cif.

Molecular Orbital Calculations. The Gaussian 03[21] software package was used to carry out DFT and TDDFT calculations using the B3LYP functional with 6-31G(d) basis sets. Structural optimization was performed on **1b** and **2b** as model compounds for simplicity.

General Synthesis. To a 1,2,4-trichlorobenzene solution (8.0 mL) of 1,2-naphthalenedicarbonitrile (357 mg, 2.0 mmol) was added a 1.0 M xylene solution of boron trichloride (2.0 mL, 1.0 equiv) at room temperature. The resultant mixture was gradually heated at 215 °C, and the temperature was maintained for 3 h. After removal of the solvent, an excess amount of phenol (>150 mg) was added, and the mixture was heated at 120 °C for 2 h. The resultant solid was extracted with toluene using a Soxhlet apparatus, to give a violet solid containing unreacted 1, 2-naphthalenedicarbonitrile and phenol, which were removed by sublimation at 140 °C under vacuum. The resultant mixture was chromatographed on a flash silica gel (Silica gel 60H for thin layer chromatography, Merck), to purify two structural isomers, **1c** (6.8 mg, 0.01 mmol, 1.6%) and **2c** (24.3 mg, 0.04 mmol, 5.7%) by using a 1:1 (v/v) mixture of $CHCl_3$ and hexane as eluent. Axially *p*-bromophenoxy substituted 1,2-subnaphthalocyanine was similarly synthesized and purified. The yields of **1d** and **2d** were 1.7% (8.7 mg) and 12.6% (60.5 mg), respectively.

Axially Phenoxy Substituted 1,2-Subnaphthalocyanine 1c. ^{1}H NMR (600 MHz, $CDCl_3$, 298 K): δ = 10.13 (d, J = 8.50 Hz, 3H), 8.91 (d, J = 8.50 Hz, 3H), 8.27 (d, J = 8.50 Hz, 3H), 8.13 (d, J = 7.96 Hz, 3H), 8.00 (m, 3H), 7.77 (m, 3H), 6.76 (m, 2H; *m*-phenoxy), 6.62 (t, J = 7.30 Hz, 1H; *p*-phenoxy), and 5.47 ppm (d, J = 8.62 Hz, 2H; *o*-phenoxy); UV/vis ($CHCl_3$): λ_{max} [nm] (ε) = 291 (62 700), 346 (17 300), 388 (20 000), and 575 (91 200 M^{-1} cm^{-1}); HR-ESI-TOF-MS: m/z (%): 661.1914 (100); Calcd for $C_{42}H_{23}N_6O_1B_1Na_1$ [M^+ + Na], 661.1919.

Scheme 1. Synthesis of 1,2-Subnaphthalocyanines[a]

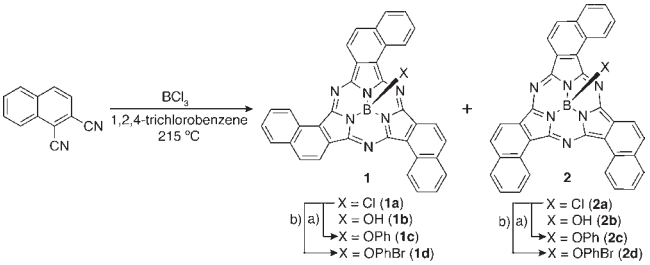

[a] Reaction conditions: (a) phenol, 120 °C, 2 h; (b) *para*-bromophenol, 120 °C, 2 h.

Axially Phenoxy Substituted 1,2-Subnaphthalocyanine 2c. ^{1}H NMR (600 MHz, $CDCl_3$, 298 K): δ = 10.19 (d, J = 8.20 Hz, 1H), 10.18 (d, J = 8.50 Hz, 1H), 10.13 (d, J = 8.62 Hz, 1H), 8.90 (d, J = 8.50 Hz, 1H), 8.87 (d, J = 8.50 Hz, 1H), 8.86 (d, J = 8.50 Hz, 1H), 8.26 (d, J = 8.32 Hz, 1H), 8.25 (d, J = 8.50 Hz, 2H), 8.12 (d, J = 7.61 Hz, 1H), 8.11 (d, J = 7.96 Hz, 2H), 8.03 (m, 2H), 7.99 (m, 1H), 7.76 (m, 3H), 6.76 (m, 2H; *m*-phenoxy), 6.62 (t, J = 7.31 Hz, 1H; *p*-phenoxy), and 5.47 ppm (d, J = 8.60 Hz, 2H; *o*-phenoxy); UV/vis ($CHCl_3$): λ_{max} [nm] (ε) = 290 (77 600), 342 (19 800), 390 (20 600), and 575 (96 600 M^{-1} cm^{-1}); HR-ESI-TOF-MS: m/z (%): 661.1915 (100) [M^+]; Calcd for $C_{42}H_{23}N_6O_1B_1Na_1$ [M^+ + Na], 661.1919.

Axially *p*-Bromophenoxy Substituted 1,2-Subnaphthalocyanine 1d. ^{1}H NMR (400 MHz, $CDCl_3$, 298 K): δ = 10.13 (d, J = 8.05 Hz, 3 H), 8.91 (d, J = 8.55 Hz, 3 H), 8.28 (d, J = 8.30 Hz, 3 H), 8.13 (d, J = 8.05 Hz, 3 H), 8.00 (t, J = 7.05 Hz, 3 H), 7.77 (t, J = 8.05 Hz, 3 H), 6.85 (d, J = 9.06 Hz, 2 H; *m*-phenoxy), 5.35 ppm (d, J = 8.81 Hz, 2 H; *o*-phenoxy); UV/vis ($CHCl_3$): λ_{max} [nm] (ε) = 291 (69 500), 347 (18 700), 389 (22 100), 534 (27 900), and 576 (97 000 M^{-1} cm^{-1}); HR-ESI-TOF-MS: m/z (%): 739.1020 (100); Calcd for $C_{42}H_{22}BBrN_6NaO^+$ [M^++ Na], 739.1024.

Axially *p*-Bromophenoxy Substituted 1,2-Subnaphthalocyanine 2d. ^{1}H NMR (400 MHz, $CDCl_3$, 298 K): δ = 10.18−10.11 (m, 3 H), 8.91−8.85 (m, 3 H), 8.32−8.25 (m, 3 H), 8.18−8.10 (m, 3 H), 8.06−7.97 (m, 3 H), 7.85−7.74 (m, 3 H), 6.85 (d, J = 8.80 Hz, 2 H; *m*-phenoxy), 5.35 ppm (d, J = 8.56 Hz, 2 H; *o*-phenoxy); UV/vis ($CHCl_3$): λ_{max} [nm] (ε) = 291 (79 600), 343 (19 900), 391 (21 000), and 575 (96 900 M^{-1} cm^{-1}); HR-ESI-TOF-MS: m/z (%): 739.1019 (100); Calcd for $C_{42}H_{22}BBrN_6NaO^+$ [M^+ + Na], 739.1024.

RESULTS AND DISCUSSION

Synthesis and Characterization. 1,2-SubNcs (**1** and **2**) were synthesized from 1,2-naphthalenedicarbonitrile and boron trichloride under conventional reaction conditions (Scheme 1).[3] Separation of the diastereomers (**1a** and **2a**) was prevented by considerable tailing of axially hydroxy-substituted species (**1b** and **2b**), which were generated in the silica gel column. In order to improve the column separation, an axial ligand exchange reaction using phenol was performed prior to the separation (Scheme 1). This enabled us to complete separation of **1c** and **2c** in 1.6% and 5.7% yields, which were not poor considering that

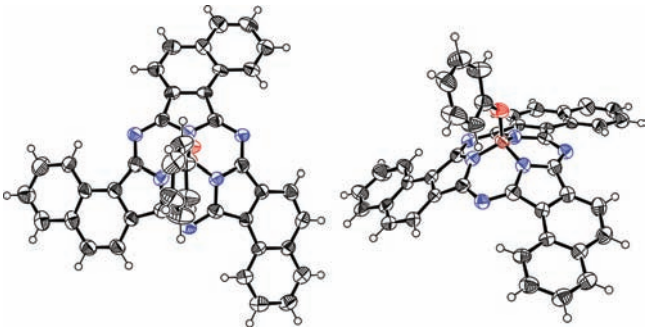

Figure 1. X-ray crystal structure of **1c**, top view (left) and side view (right). The thermal ellipsoids are scaled to the 50% probability level.

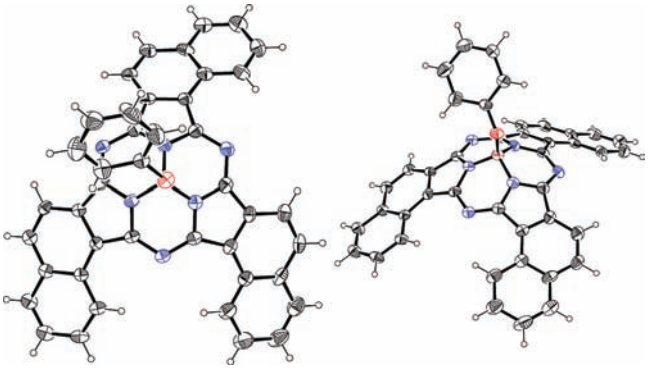

Figure 2. X-ray crystal structure of **2c**, top view (left) and side view (right). The thermal ellipsoids are scaled to the 50% probability level.

approximately 70% of the starting 1,2-naphthalenedicarbonitrile was recovered. Axially *p*-bromophenoxy-substituted 1,2-SubNcs, **1d** and **2d**, were similarly obtained in 1.7% and 12.6% yields, respectively, using *p*-bromophenol in the last step of the reaction (Scheme 1).

Compounds **1c** and **2c** were first characterized by high-resolution electrospray ionization mass spectrometry (HR-ESI-MS), with the observed molecular ion peaks at 661.1914 for **1c** and at 661.1915 for **2c** (calcd for $C_{42}H_{23}N_6O_1B_1Na_1$ = 661.1919 [M^+ + Na]). Successful replacement of the axial chlorine ligand with *p*-bromophenoxy substituents was also confirmed by HR-ESI-MS. The ^{1}H NMR spectrum of **1c** in $CDCl_3$ exhibits naphthalene proton peaks as a doublet at 10.13, 8.91, 8.27, and 8.13 ppm and as a triplet at 8.00 and 7.77 ppm due to the C_3 symmetric structure, whereas the ^{1}H NMR spectrum of **2c** in $CDCl_3$ shows six pairs of either doublets or triplets at similar chemical shifts to those of **1c** because of the lower C_1 symmetric structure (Figure S1 in the Supporting Information (SI)). In both cases, peaks of the axial phenoxy substituent are observed at 6.76, 6.62, and 5.47 ppm due to the diatropic ring current effects arising from the 14π-electron conjugation systems.[3] The ^{1}H NMR measurements on **1d** and **2d** revealed similar signal patterns to those of **1c** and **2c** (Figure S2 in the SI).

Crystal Structures of 1c and 2c. Crystals of **1c** and **2c** suitable for single crystal X-ray analysis were grown by slow diffusion of 2-propanol into $CHCl_3$ solutions of **1c** and **2c**. Since **1c** and **2c** are racemic mixtures, both enantiomers are observed in the unit cells (Figure S3 in the SI), and only clockwise isomers are depicted in Figures 1 and 2. Three peripheral naphthalene

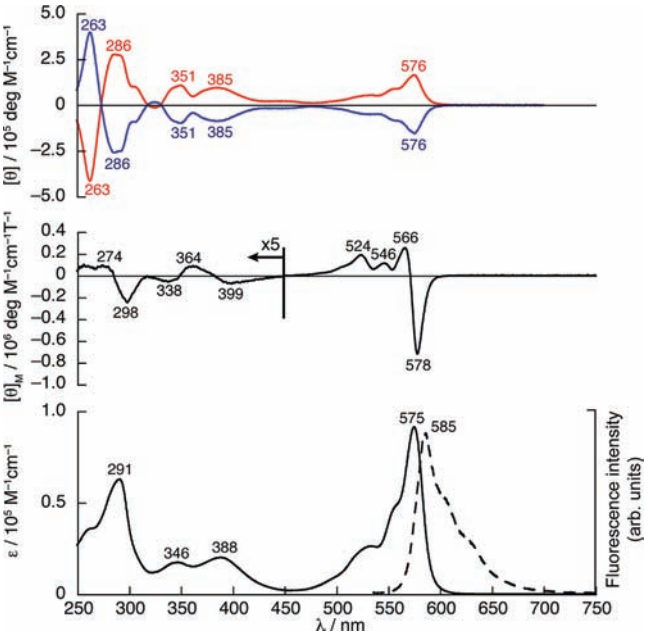

Figure 3. UV/vis absorption (bottom) and MCD (middle) spectra of **1c**, and CD (top) spectra of **1cFr1** (blue) and **1cFr2** (red) in $CHCl_3$. Fluorescence spectrum in $CHCl_3$ is shown as a dashed line (bottom).

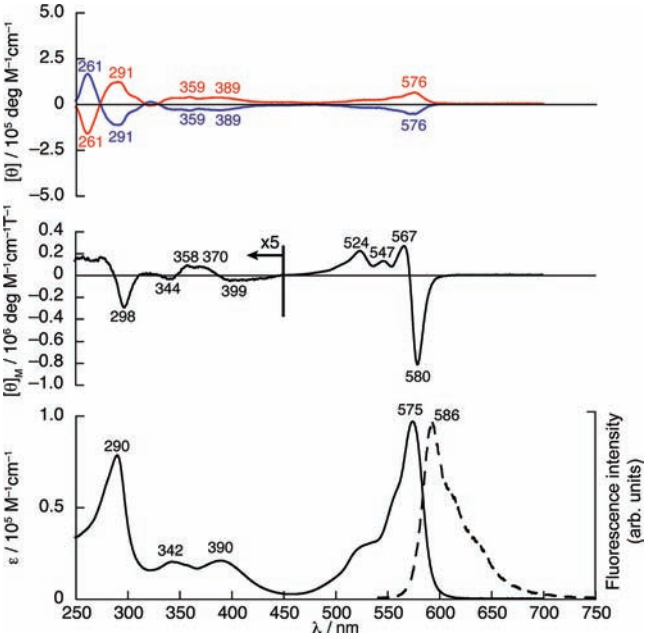

Figure 4. UV/vis absorption (bottom) and MCD (middle) spectra of **2c**, and CD (top) spectra of **2cFr1** (blue) and **2cFr2** (red) in $CHCl_3$. Fluorescence spectrum in $CHCl_3$ is shown as a dashed line (bottom).

moieties of **1c** are arranged in a clockwise manner, whereas one of these points in the opposite direction in the case of **2c**. Similar to conventional SubPcs, both **1c** and **2c** adopt bowl-shaped conformations with a boron atom at the center coordinated in a tetrahedral fashion. The bowl depths defined by the deviation of the boron atom from the mean plane of the three coordinating nitrogen atoms (3N-mean plane) are 0.60 Å for **1c**

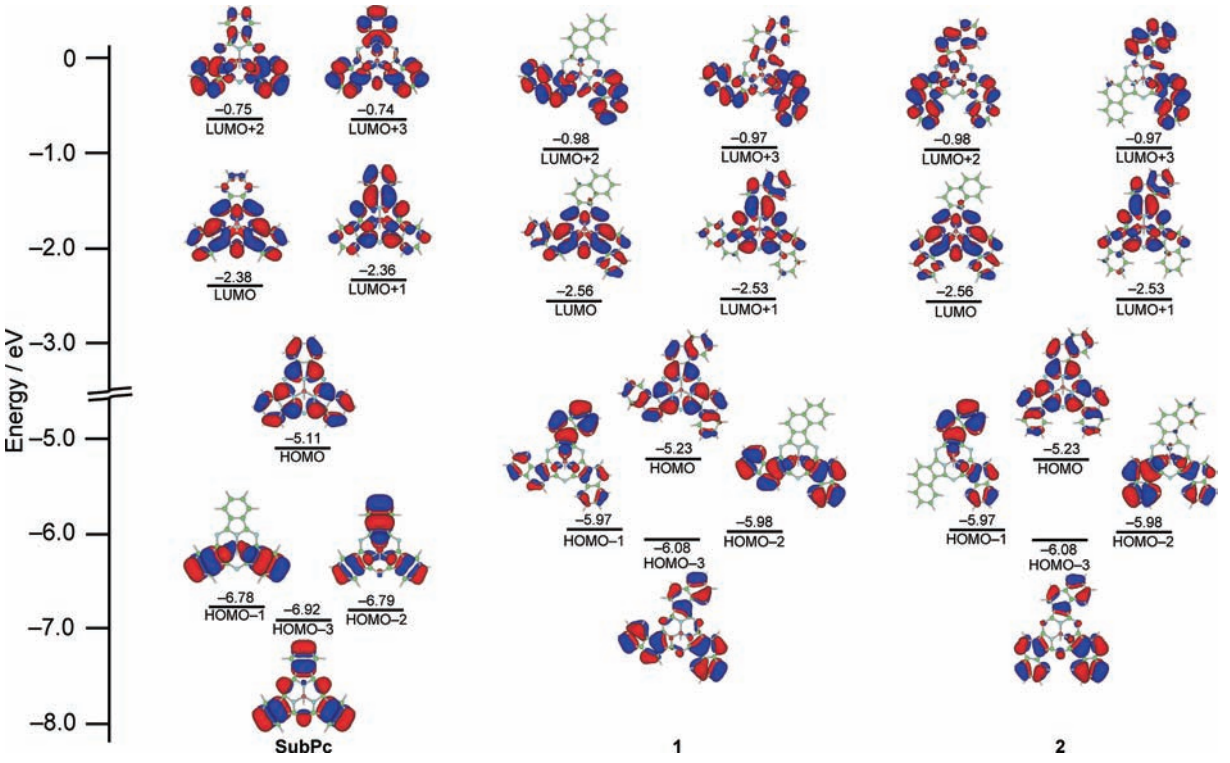

Figure 5. Partial molecular orbital diagram of **SubPc** (left), **1** (middle), and **2** (right).

and 0.63 Å for **2c**, both of which are in the range of those of conventional SubPcs.[3]

Electronic Absorption, Magnetic Circular Dichroism, and Emission Spectra. Apart from some differences in the shoulder-like absorptions at ca. 530 and 560 nm, the absorption spectra of **1c** and **2c** have essentially similar shapes, including values of the molar absorption coefficient as well as positions of the main absorptions at 575, 388, 346, and 291 nm for **1c** and at 575, 390, 342, and 290 nm for **2c** (Figures 3 and 4). Compared to unsubstituted SubPc,[3] the Q-bands of **1c** and **2c** (575 nm) are shifted slightly to the red, by 10 nm, although a significantly larger red shift of 95 nm is seen for 2,3-subnaphthalocyanine (2,3-SubNc).[22] This slight change in the shape and position of the Q-band absorption is similar to that of 1,2-naphthalocyanines from normal Pcs.[19] In contrast to the small change in the Q-band region, a significant difference from conventional SubPcs is observed in the region of 250−450 nm. The absorption spectra of SubPc molecules generally comprises two main broad bands in the Soret-band region,[3,23] whereas **1c** and **2c** exhibit three bands at 388, 346, and 291 nm, and at 390, 342, and 290 nm, respectively.

MCD measurements were performed on **1c** and **2c** (Figures 3 and 4) in order to obtain additional information on the electronic structures. The MCD spectra of both **1c** and **2c** exhibit similar spectral features over the entire region, where dispersion-type signals are observed corresponding to the Q-bands, with negative to positive envelopes at 578 and 566 nm for **1c** and at 580 and 567 nm for **2c**. Based on the molecular symmetries of C_3 and C_1, these MCD signals can be assigned as a Faraday *A* term for **1c** and a pseudo Faraday *A* term for **2c**. A pseudo Faraday *A* term is generally observed when two Faraday *B* terms lie close in energy, which occurs when Pc analogues with low symmetry accidentally have nearly degenerate excited states.[24−26] In the current case, the MCD signals in the Q-band region of **1c** are theoretically regarded as a Faraday A term, but in order to facilitate comparison of the observed oscillator and rotational strengths between **1c** and **2c**, the Faraday *A* term is expressed with two closely lying Faraday *B* terms (i.e., as a pseudo Faraday *A* term) in the following discussion. In the 250−450 nm region, several MCD signals are observed corresponding to the characteristic absorptions of 1,2-SubNcs. A dispersion type MCD trough (399 nm) and peak (364 nm) associated with the broad absorption at 388 nm for **1c**, and a similar MCD peak and trough at 370 and 399 nm associated with the absorption peak at 390 nm for **2c**, indicate the presence of transitions to nearly degenerate excited states. In addition to the variation in shape of the absorption spectra from those of SubPcs in the higher energy region, these MCD signals imply that the annulation of benzene rings at the α- and β-positions of SubPc causes significant changes in the energy levels of molecular orbitals (MOs) lying below the HOMO and above the LUMO+1. Details of this are discussed in the following section, based on theoretical calculations.

Both compounds **1c** and **2c** exhibit intense mirror-imaged emissions at 585 and 586 nm, respectively, upon excitation at 495 nm (Figures 3 and 4). The Stokes shifts of **1c** and **2c** are 297 and 326 cm^{-1}, and the fluorescence quantum yields and lifetimes are 0.14 and 2.1 ns for **1c** and 0.11 and 2.1 ns for **2c**.[27] These values are very similar to those of SubPcs reported to date.[3]

Electronic Structures and Theoretical Absorption Spectra. Structural optimization using **1b** and **2b** as theoretical models was performed based on the DFT method at the B3LYP/6-31G(d) level, while time-dependent (TD) DFT calculation was also carried out at the same level. As a reference, DFT and TDDFT calculations were also performed on a model compound of unsubstituted SubPc having an OH group as an axial ligand. In the frontier MOs, **1** and **2** essentially exhibit a

Table 1. Selected Transition Energies and Wave Functions of 1, 2, and SubPc Calculated Based on the TDDFT (B3LYP/6-31G(d)) Method

compd	energy [nm]	f[a]	R(velocity)[b]	wave function[d]
1	511	0.36	−51.6 (C)[c] 51.4 (AC)[c]	+ 0.621|146 ← 145> − 0.114|147 ← 138> + 0.167|147 ← 142> + ...
	508	0.35	−49.5 (C) 49.7 (AC)	+ 0.621|147 ← 145> + 0.116|146 ← 138> − 0.172|146 ← 142> + ...
	399	0.24	−52.5 (C) 53.1 (AC)	+ 0.636|146 ← 142> − 0.149|147 ← 143> − 0.128|146 ← 144> + 0.112|147 ← 145> + ...
	395	0.24	−48.9 (C) 48.7 (AC)	+ 0.658|147 ← 142> − 0.101|146 ← 143> − 0.104|146 ← 145> + ...
2	515	0.28	−11.3 (C) 11.3 (AC)	+ 0.622|146 ← 145> − 0.125|147 ← 138> − 0.150|147 ← 142> + ...
	505	0.42	−20.3 (C) 20.3 (AC)	+ 0.615|147 ← 145> + 0.126|146 ← 138> + 0.171|146 ← 142> + ...
	403	0.20	−19.5 (C) 19.5 (AC)	+ 0.591|146 ← 142> − 0.104|146 ← 138> + 0.125|147 ← 142> − 0.250|146 ← 144> − 0.118|147 ← 145> + ...
	397	0.20	−17.7 (C) 17.7 (AC)	+ 0.634|147 ← 142> − 0.163|146 ← 143> − 0.112|147 ← 143> + ...
SubPc	489	0.31		+ 0.617|107 ← 106> − 0.109|108 ← 100> + 0.176|108 ← 103> + ...
	486	0.31		+ 0.618|108 ← 106> + 0.111|107 ← 100> − 0.177|107 ← 103> + ...
	299	0.26		+ 0.224|107 ← 98> + 0.225|108 ← 99> + 0.361|107 ← 101> + 0.289|108 ← 102> − 0.319|107 ← 103> + 0.100|107 ← 104> + 0.112|108 ← 105> − 0.105|109 ← 106> + ...
	297	0.24		+ 0.225|108 ← 98> − 0.196|107 ← 99> + 0.163|108 ← 100> + 0.435|108 ← 101> − 0.123|107 ← 102> + 0.353|108 ← 103> + ...

[a] Oscillator strength. [b] Rotational strength in 10^{-40} cgs. [c] C and AC represent a clockwise and an anticlockwise isomer, respectively. [d] The wave functions are based on the eigenvectors predicted by TDDFT. The |145> and |106> represent the HOMO of **1** and **2** and that of **SubPc**, respectively. Eigenvectors greater than 0.10 are included.

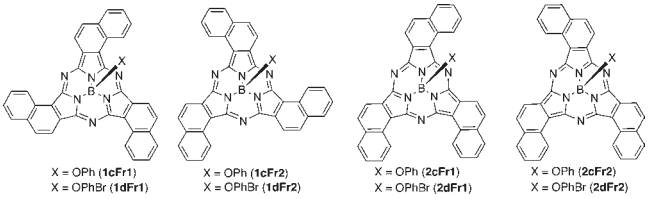

Figure 6. Diastereomers and enantiomers of 1,2-subnaphthalocyanines.

similar electron density distribution pattern to that of SubPc, and delocalization of electron density on the exterior benzene rings is also observed for both **1** and **2** (Figure 5). The energy levels of the HOMO and the first and second LUMOs are slightly stabilized compared to those of SubPc. The HOMO−LUMO energy gaps of **1** and **2** are both 2.67 eV, which is smaller than that of SubPc (2.73 eV). In-depth analyses on the MOs above the LUMO+1 and below the HOMO reveal a slight stabilization of the degenerate LUMO+2 and LUMO+3 and significant destabilization of the HOMO−1—HOMO−3 compared to SubPcs.

The TDDFT calculation estimated the Q bands to lie at 511 and 508 nm for **1** and at 515 and 505 nm for **2**, which comprise transitions from the HOMO to the nearly degenerate LUMO and LUMO+1, and these values are shifted slightly to the red compared to SubPcs (489 and 486 nm, Table 1). These results are in good agreement with the observed small red shift of the Q-band in the absorption spectra and the associated dispersion-type MCD signals. In the case of SubPcs, the bands next to the Q-bands were calculated to lie at 299 and 297 nm, assigned to transitions from MOs below the HOMO to the degenerate LUMO and LUMO+1, whereas the corresponding bands of **1** at 399 and 395 nm and of **2** at 403 and 397 nm comprise transitions mainly from the HOMO−3 to the LUMO and LUMO+1 (Table 1). As a result of the small degree of mixing of bands in this region, dispersion-type signals are clearly observed in the MCD spectra, corresponding to the absorptions at 388 (**1c**) and 390 (**2c**) nm. These results indicate that the main change due to the oblique annulation of benzene rings at the α- and β-positions of SubPc is destabilization of the HOMO−3. Thus, the two weak bands at ca. 350−430 nm and the single intense band at ca. 290 nm in the observed absorption spectra are characteristic of the electronic absorption spectra of 1,2-SubNcs, while conventional SubPcs and 2,3-SubNcs only exhibit two broad bands in the same region.[3,22,23]

Chiral Separation and Circular Dichroism Spectra. Optical resolution of **1c** and **2c** was performed on an HPLC equipped with a chiral column using a mixture of CH_2Cl_2 and hexane (1:1 (v/v) for **1c** and 1:3 (v/v) for **2c**), and two fractions were obtained (**1cFr1** and **1cFr2**, and **2cFr1** and **2cFr2**, Figure 6 and Figure S5 in the SI). In the CD spectra, the first fractions, **1cFr1** and **2cFr1**, show a negative sign between 275 and 600 nm and a positive sign in the higher energy region, whereas the second fractions, **1cFr2** and **2cFr2**, show mirror-imaged positive and negative signs in the corresponding regions (Figures 3 and 4). Band deconvolution analysis[28] was performed on the absorption,

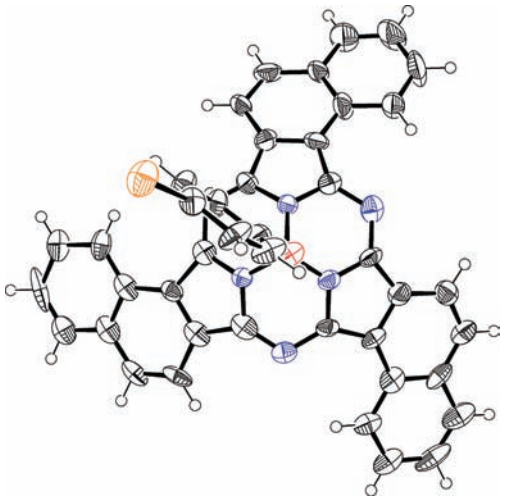

Figure 7. X-ray crystal structure of **1dFr1**. The thermal ellipsoids are scaled to the 50% probability level.

CD, and MCD spectra in the Q-band region in order to estimate the rotational strengths from the observed spectra (Figures S6 and S7 in the SI). Eleven and twelve components, respectively, were used to fit the region between 450 and 650 nm for **1cFr1** and **2cFr1**. The experimental rotational strengths (R_{obsd}) and oscillator strengths (f_{obsd}) of the Q_{00}-bands were estimated using eqs 1 and 2,[29,30] in which μ, h, m, ν, N, and c represent the transition electric dipole moment, Planck's constant, the electron mass, the frequency at which absorption occurs, Avogadro's number, and the speed of light in a vacuum, respectively. The experimental rotational strengths of **1cFr1** (-5.85×10^{-39} and -5.19×10^{-39} cgs) are about three times larger than those of **2cFr1** (-2.08×10^{-39} and -2.06×10^{-39} cgs), whereas the experimental oscillator strengths of **1c** (0.13 and 0.12) are similar to those of **2c** (0.14 and 0.13).

$$f_{obsd} = \frac{8\pi^2 m\nu}{3he^2}|\mu|^2 = 0.476 \times 10^{30}\nu|\mu|^2 \quad (1)$$

$$R_{obsd} = \frac{hc}{48\pi^2 N}\int \frac{\theta(\nu)}{\nu}\,d\nu \approx 0.696 \times 10^{-42}\int \frac{\theta(\nu)}{\nu}\,d\nu \quad (2)$$

In principle, the CD intensity (rotational strength R) of chiral molecules is expressed by the Rosenfeld equation.[30]

$$R = \mathrm{Im}(\mu \cdot m) \quad (3)$$

In this equation, μ and m are a transition electric dipole moment and a transition magnetic dipole moment, respectively, and Im denotes the imaginary part of $\mu \cdot m$. Since oscillator strengths (f_{obsd}) are proportional to μ based on eq 1, **1c** and **2c** can be expected to have similar values of transition electric dipole moments. Thus the smaller rotational strengths (R_{obsd}) of **2c** compared to those of **1c** can be ascribed to the smaller transition magnetic dipole moments of **2c** as compared with those of **1c**. Considering that circular redistribution of charges in transitions generates transition magnetic dipole moments, it appears plausible that one oppositely arranged naphthalene moiety in **2c** reduces the net m values of **2c** to one-third of those of **1c**.

The theoretical CD spectra based on TDDFT calculations provide an initial clue for assigning absolute structures. Model compounds with a clockwise arrangement of benzene rings exhibit negative CD bands in the Q-band region, while, inversely, those with an anticlockwise arrangement show positive CD bands (Table 1 and Figures S8 and S9 in the SI). The theoretical CD spectra also reproduce the intensity difference between compounds **1** and **2**.

Absolute Structure of 1d Elucidated by X-ray Crystallographic Analysis. Enantiomers of axially *p*-bromophenoxy-substituted species **1d** and **2d**, i.e. **1dFr1** and **1dFr2**, and **2dFr1** and **2dFr2** (Figure 6), were similarly obtained by optical resolution using the HPLC technique. These isomers exhibit similar CD spectra to those of **1c** and **2c** (Figure S10 in the SI). Suitable crystals of **1dFr1** were obtained by slow diffusion of methanol into a toluene solution, and the crystal structure was unambiguously elucidated by single crystal X-ray analysis (Figure 7 and Figure S4 in the SI). The crystal structure of **1dFr1** indicates a clockwise arrangement of the naphthalene moieties when viewed from the axial position of the boron atom. This result is in good agreement with the predicted molecular structure based on the theoretical CD calculation. The negative CD signs in the Q-band region are thus indicative of the clockwise isomer, whereas the positive signs indicate an anticlockwise isomer (**1dFr2** in Figure 6). Since the CD signal is determined by the orientation of the naphthalene moieties, the structure−chirality relationship obtained for **1d** appears also true for **2d**. Moreover, it can be reasonably claimed that this relationship will be applicable to **1c** and **2c**, since the axial ligands have only a minor influence on the absorption spectra and chirality of the molecules.

■ CONCLUSIONS

In summary, the separation and characterization of all of the diastereomers and enantiomers of 1,2-SubNcs was achieved successfully, the first example in the chemistry of inherently chiral SubPcs. Electronic absorption and MCD measurements, in addition to theoretical calculation, reveal that the oblique annulation of the benzene rings to SubPc causes minor alterations in the energy levels of the HOMO, LUMO, and LUMO+1 but major changes in the HOMO−3, which leads to the appearance of characteristic bands in the Soret band region. The CD spectra of chiral 1,2-SubNcs exhibited similar shapes to those of the absorption spectra apart from their signs, and the smaller rotational strengths of enantiomers of **2c** compared to those of **1c** were also observed, which can be ascribed to the reduction of transition magnetic dipole moments of **2** by the one oppositely arranged naphthalene moiety in **2**. The absolute structure of **1dFr1** led us to a comprehensive understanding of the structure−chirality relationship of 1,2-SubNcs; i.e. the negative CD signs in the Q-band region are indicative of a molecular structure where the naphthalene moieties are arranged clockwise, while the positive CD signs in that region indicate an anticlockwise arrangement. The discussion in this article is useful for the analyses of the structure−chirality relationship of the other chiral SubPcs and, moreover, indispensable, considering the potential utility of this three-dimensional chirality for future applications.

■ ASSOCIATED CONTENT

Supporting Information. ^{1}H NMR, UV/vis absorption, MCD, and CD spectra, crystal packing diagrams, chiral HPLC

chromatograms, theoretical absorption and CD spectra, results of the band deconvolution analyses, and complete ref 21. This material is available free of charge via the Internet at http://pubs.acs.org.

AUTHOR INFORMATION

Corresponding Author
nagaok@m.tohoku.ac.jp; t.nyokong@ru.ac.za

ACKNOWLEDGMENT

This work was partly supported by a Grant-in-Aid for bilateral program promoted by Japan Society for the Promotion of Science (JSPS) and National Research Foundation (NRF) of South Africa, a Grant-in-Aid for Scientific Research on Innovative Areas (No. 20108007, "pi-Space") from the Ministry of Education, Culture, Sports, Science, and Technology (MEXT), and a Grant-in-Aid for Scientific (C) (No. 23550040) from JSPS. We also thank NRF of South Africa for funding (Grant number: 72195). The authors thank Dr. Eunsang Kwon in Tohoku University for X-ray analysis, and Prof. Takeaki Iwamono and Dr. Shintaro Ishida in Tohoku University for X-ray measurement.

REFERENCES

(1) Meller, A.; Ossko, A. *Monatsh. Chem.* **1972**, *103*, 150.
(2) Kietaibl, H. *Monatsh. Chem.* **1974**, *105*, 405.
(3) Claessens, C. G.; Gonzalez-Rodriguez, D.; Torres, T. *Chem. Rev.* **2002**, *102*, 835.
(4) (a) Claessens, C. G.; Gonzalez-Rodriguez, D.; Torres, T.; Martin, G.; Agullo-Lopez, F.; Ledoux, I.; Zyss, J.; Ferro, V. R.; de la Vega, J. M. G. *J Phys. Chem. B* **2005**, *109*, 3800. (b) Dini, D.; Vagin, S.; Hanack, M.; Amendola, V.; Meneghetti, M. *Chem. Commun.* **2005**, 3796.
(5) (a) Medina, A. S.; Claessens, C. G.; Rahman, G. M. A.; Lamsabhi, A. M.; Mo, O.; Yanez, M.; Guldi, D. M.; Torres, T. *Chem. Commun.* **2008**, 1759. (b) Rodriguez-Morgade, M. S.; Claessens, C. G.; Medina, A.; Gonzalez-Rodriguez, D.; Gutierrez-Puebla, E.; Monge, A.; Alkorta, I.; Elguero, J.; Torres, T. *Chem.—Eur. J.* **2008**, *14*, 1342. (c) Xu, H.; Ng, D. K. P. *Inorg. Chem.* **2008**, *47*, 7921. (d) Zhao, Z. X.; Cammidge, A. N.; Cook, M. J. *Chem. Commun.* **2009**, 7530. (e) Ziessel, R.; Ulrich, G.; Elliott, K. J.; Harriman, A. *Chem.—Eur. J.* **2009**, *15*, 4980. (f) Morse, G. E.; Paton, A. S.; Lough, A.; Bender, T. P. *Dalton. Trans.* **2010**, *39*, 3915.
(6) (a) Heremans, P.; Cheyns, D.; Rand, B. P. *Acc. Chem. Res.* **2009**, *42*, 1740. (b) Gommans, H.; Aernouts, T.; Verreet, B.; Heremans, P.; Medina, A.; Claessens, C. G.; Torres, T. *Adv. Funct. Mater.* **2009**, *19*, 3435. (c) Gommans, H.; Cheyns, D.; Aernouts, T.; Girotto, C.; Poortmans, J.; Heremans, P. *Adv. Funct. Mater.* **2007**, *17*, 2653. (d) Das, B.; Tokunaga, E.; Shibata, N.; Kobayashi, N. *J. Fluorine Chem.* **2010**, *131*, 652. (e) Verreet, B.; Schols, S.; Cheyns, D.; Rand, B. P.; Gommans, H.; Aernouts, T.; Heremans, P.; Genoe, J. *J. Mater. Chem.* **2009**, *19*, 5295. (f) Pakhomov, G. L.; Travkin, V. V.; Bogdanova, A. Y.; Guo, T. F. *J. Porphyrins Phthalocyanines* **2008**, *12*, 1182. (g) Rio, Y.; Vazquez, P.; Palomares, E. *J. Porphyrins Phthalocyanines* **2009**, *13*, 645. (h) Tong, X. R.; Lassiter, B. E.; Forrest, S. R. *Org. Electron.* **2010**, *11*, 705.
(7) (a) Yasuda, T.; Tsutsui, T. *Mol. Cryst. Liq. Cryst.* **2007**, *462*, 3. (b) Klaus, D.; Knecht, R.; Dragasser, A.; Keil, C.; Schlettwein, D. *Phys. Status Solidi A* **2009**, *206*, 2723. (c) Mattheus, C. C.; Michaelis, W.; Kelting, C.; Durfee, W. S.; Wohrle, D.; Schlettwein, D. *Synth. Met.* **2004**, *146*, 335.
(8) (a) Gonzalez-Rodriguez, D.; Carbonell, E.; Guldi, D. M.; Torres, T. *Angew. Chem., Int. Ed.* **2009**, *48*, 8032. (b) Iglesias, R. S.; Claessens, C. G.; Rahman, G. M. A.; Herranz, M. A.; Guldi, D. M.; Torres, T. *Tetrahedron* **2007**, *63*, 12396. (c) Gonzalez-Rodriguez, D.; Torres, T.; Guldi, D. M.; Rivera, J.; Echegoyen, L. *Org. Lett.* **2002**, *4*, 335. (d) Iglesias, R. S.; Claessens, C. G.; Torres, T.; Rahman, G. M. A.; Guldi, D. M. *Chem. Commun.* **2005**, 2113.
(9) (a) Kim, J. H.; El-Khouly, M. E.; Araki, Y.; Ito, O.; Kay, K. Y. *Chem. Lett.* **2008**, *37*, 544. (b) El-Khouly, M. E.; Ju, D. K.; Kay, K. Y.; D'Souza, F.; Fukuzumi, S. *Chem.—Eur. J.* **2010**, *16*, 6193. (c) El-Khouly, M. E.; Shim, S. H.; Araki, Y.; Ito, O.; Kay, K. Y. *J. Phys. Chem. B* **2008**, *112*, 3910.
(10) (a) Claessens, C. G.; Torres, T. *J. Am. Chem. Soc.* **2002**, *124*, 14522. (b) Claessens, C. G.; Torres, T. *Chem. Commun.* **2004**, 1298.
(11) Shimizu, S.; Nakano, S.; Hosoya, T.; Kobayashi, N. *Chem. Commun.* **2011**, *47*, 316.
(12) (a) Claessens, C. G.; Torres, T. *Tetrahedron Lett.* **2000**, *41*, 6361. (b) Claessens, C. G.; Torres, T. *Chem.—Eur. J.* **2000**, *6*, 2168. (c) Claessens, C. G.; Torres, T. *Eur. J. Org. Chem.* **2000**, 1603.
(13) Kobayashi, N.; Nonomura, T. *Tetrahedron Lett.* **2002**, *43*, 4253.
(14) Higashibayashi, S.; Sakurai, H. *J. Am. Chem. Soc.* **2008**, *130*, 8592.
(15) Thilgen, C.; Diederich, F. *Chem. Rev.* **2006**, *106*, 5049.
(16) (a) Dukovic, G.; Balaz, M.; Doak, P.; Berova, N. D.; Zheng, M.; Mclean, R. S.; Brus, L. E. *J. Am. Chem. Soc.* **2006**, *128*, 9004. (b) Peng, X.; Komatsu, N.; Bhattacharya, S.; Shimawaki, T.; Aonuma, S.; Kimura, T.; Osuka, A. *Nat. Nanotechnol.* **2007**, *2*, 361.
(17) Kobayashi, N.; Narita, F.; Ishii, K.; Muranaka, A. *Chem.—Eur. J.* **2009**, *15*, 10173.
(18) Flack, H. D.; Bernardinelli, G. *J. Appl. Crystallogr.* **2000**, *33*, 1143.
(19) (a) Hanack, M.; Renz, G.; Strahle, J.; Schmid, S. *J. Org. Chem.* **1991**, *56*, 3501. (b) Negrimovskii, V. M.; Bouvet, M.; Luk'yanets, E. A.; Simon, J. *J. Porphyrins Phthalocyanines* **2000**, *4*, 248. (c) Gacho, E. H.; Naito, T.; Inabe, T.; Fukuda, T.; Kobayashi, N. *Chem. Lett.* **2001**, 260. (d) Gacho, E. H.; Imai, H.; Tsunashima, R.; Naito, T.; Inabe, T.; Kobayashi, N. *Inorg. Chem.* **2006**, *45*, 4170.
(20) Sheldrick, G. M. *SHELXL-97, Program for the Solution and Refinement of Crystal Structures*; University of Göttingen: Göttingen, Germany, 1997.
(21) Frisch, M. J. et al. *Gaussian 03*; Gaussian, Inc.: Pittsburgh, PA, 2003.
(22) (a) Rauschnabel, J.; Hanack, M. *Tetrahedron Lett.* **1995**, *36*, 1629. (b) Zyskowski, C. D.; Kennedy, V. O. *J. Porphyrins Phthalocyanines* **2000**, *4*, 707. (c) Nonell, S.; Rubio, N.; del Rey, B.; Torres, T. *J. Chem. Soc., Perkin Trans. 2* **2000**, *6*, 1091.
(23) Kobayashi, N.; Ishizaki, T.; Ishii, K.; Konami, H. *J. Am. Chem. Soc.* **1999**, *121*, 9096.
(24) Stillman, M. J.; Nyokong, T. In *Phthalocyanines: Properties and Applications*; Leznoff, C. C., Lever, A. B. P., Eds.; Wiley-VCH: New York, 1989−1996; Vol. 1, pp 133−289.
(25) Mack, J.; Stillman, M. J.; Kobayashi, N. *Coord. Chem. Rev.* **2007**, *251*, 429.
(26) (a) Kaito, A.; Nozawa, T.; Yamamoto, T.; Hatano, M.; Orii, Y. *Chem. Phys. Lett.* **1977**, *52*, 154. (b) Tajiri, A.; Winkler, J. *Z. Naturforsch. A* **1983**, *38*, 1263.
(27) Quantum yields were determined relative to Rhodamine 6G (Φ_F = 0.94 in ethanol): Fischer, M.; Georges, J. *Chem. Phys. Lett.* **1996**, *260*, 115.
(28) Mack, J.; Stillman, M. J. *Coord. Chem. Rev.* **2001**, *219*, 993.
(29) Charney, E. *The Molecular Basis of Optical Activity*; Wiley: New York, 1979.
(30) Roger, A.; Norden, B. *Circular Dichroism and Liner Dichroism*; Oxford University Press: Oxford, 1997.